

White paper: Technical-scientific informative ITC-05 /ATCP

Elastic moduli characterization of wood and wood products using the Impulse Excitation Technique

ATCP Physical Engineering
Sonelastic Division
www.sonelastic.com

Authors:

Lucas Barcelos Otani (Otani, L.B.)¹

Pedro Gutemberg de Alcântara Segundinho, PhD (Segundinho, P.G.A.)²

Elen Aparecida Martines Morales, PhD (Morales, E. A. M.)³

Antônio Henrique Alves Pereira, PhD (Pereira, A.H.A.)¹

(1) ATCP Physical Engineering,

(2) Federal University of Espírito Santo,

(3) São Paulo State University

Revision 1.4
August 18th, 2017

TABLE OF CONTENTS

1. Objective	1
2. Introduction.....	1
3. Elastic moduli characterization of wood using the Impulse Excitation Technique	3
3.1. Technique fundamentals	3
3.2. Vibration modes.....	5
3.3. Elastic moduli of wood specimens	7
3.3.1 Young’s modulus.....	8
3.3.2 Shear modulus (modulus of rigidity).....	9
3.3.3 Poisson’s ratio	9
3.4. Expected values for the elastic moduli of wood	10
4. Case Study #1: Characterization of Eucalyptus bars using Sonelastic® solutions	11
4.1. Materials and methods	11
4.2. Results and discussions	13
5. Case study #2: Estimation and characterization of the Young’s modulus of a cylindrical metallic composite and of a wooden log with heartwood and sapwood	15
5.1. Fundamentals and equations	15
5.2. Materials and methods	16
5.3. Results and discussions.....	18
6. Final considerations.....	21
7. References.....	22
Appendix A – Elasticity theory applied to wood	23
Appendix B – Developing a model to predict the Young's modulus values of heartwood and sapwood in wooden cylinder.....	28
Appendix C – Frequently asked questions (FAQ)	33

1. Objective

The objective of this white paper is to introduce the theory and methodology for the non-destructive elastic moduli characterization of wood and wood products using the Impulse Excitation Technique (ASTM E1876 [1] and correlated). The study presents a literature review and the advances achieved by ATCP Physical Engineering regarding the application of this characterization technique for this class of material.

2. Introduction

Wood, both for its availability and characteristics, was one of the first materials used by man for structural means. The main function of this material is for supporting the tree structure and it may be defined as an organic solid composite majorly made of cellulose and lignin [2].

Wood materials originates from stems, which constantly grow both in diameter (growth rings) and in length (grain direction). Besides its structural function, it can be also employed as the raw material for a number of processes, for example the production of paper, furniture and charcoal.



Figure 1 - Bridge located over the Montmorency river, in the Montmorency forest, Quebec, Canada. It has a span of 44 m, height of 33 m and width of 4.8 m [3].

Because of the microstructural characteristics arising from being naturally sourced, wood presents distinct physical properties according to its orientation (anisotropy) [2]. The three main axes that characterize this material are presented in Figure 2, and are listed below:

- Longitudinal (L): parallel axis to the fibers (grain direction);
- Radial (R): normal axis to the growth rings (perpendicular to the grain in the radial direction);
- Tangential (T): perpendicular axis to the grain and tangent to the growth rings.

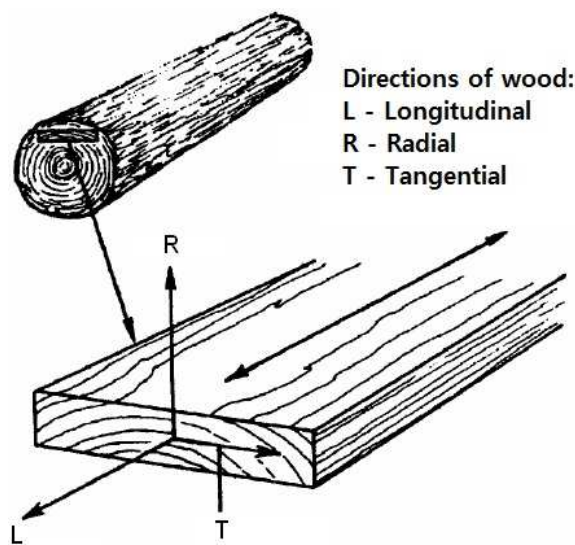


Figure 2 - The three main axes of wood with respect to the grain direction and the growth rings [4].

Wood is classified as an orthotropic material; therefore, it presents orthogonal planes of symmetry in which its properties are constants for each plane [5]. This classification, however, may be taken as a simplification because depending on the property under analysis, it is possible to verify a variation in the values along its radial direction, for instance.

The elastic properties characterization becomes important for materials such as wood because its values are used for material selection, numerical simulations, structural calculations, and to predict properties that are only obtained through destructive tests. Considering these factors, elastic moduli are also widely used for the classification and quality control of wood products.

Such applications are possible because of the sensibility of these properties to the presence of discontinuities, defects, cracks, knots, microstructural changes and chemical composition [6].

3. Elastic moduli characterization of wood using the Impulse Excitation Technique

3.1. Technique fundamentals

The Impulse Excitation Technique (ASTM E1876 [1]) essentially determines the elastic moduli of a material based on the natural vibration frequencies of a sample with regular geometry (bar, cylinder, disc or ring). These frequencies are excited by a brief mechanical impulse, followed by the acquisition of the acoustic response using a microphone. A mathematical analysis is performed on the acoustic signal in order to obtain the frequency spectrum (Fast Fourier transform). Based on this, the dynamic elastic moduli are calculated using pre-determined equations (ASTM E1876), which considers the geometry, mass, sample dimensions and frequencies obtained through the analysis [1].

For the excitation of a desired vibration mode, it is necessary to set up specific boundary conditions. Figure 3 presents a sample holder system with the impulse device and microphone positioned to measure the Young's modulus of a rectangular bar through the flexural vibration mode.

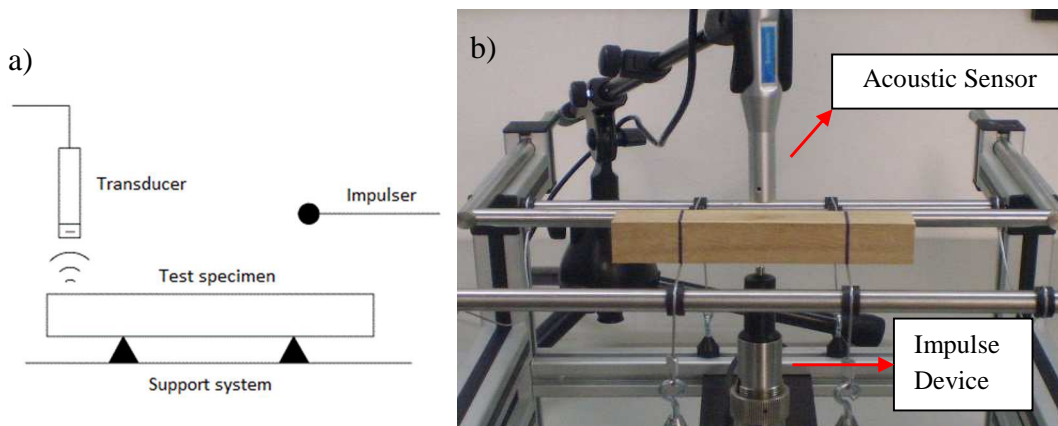


Figure 3 – a) Basic set up to characterize the flexural vibration mode of a bar using the Impulse Excitation Technique [8] and b) SA-BC support for bars and cylinders developed and manufactured by ATCP Physical Engineering.

The elastic moduli obtained by the Impulse Excitation Technique are dynamic and their correlation with the values obtained through a quasi-static test was investigated for samples of *Eucalyptus sp.* (Equation A), and *Pinus oocarpa* (Equation B) [7]. The findings of the correlation between the transversal Young's modulus obtained by a

quasi-static experiment (E_E) and the longitudinal Young's modulus dynamically obtained using the Impulse Excitation Technique (E_D), expressed in MPa, can be found next:

$$E_D = 864.75 + 0.99 E_E, \text{ for } Eucalyptus \text{ sp} \quad (\text{A})$$

$$E_D = 310.15 + 1.07 E_E, \text{ for } Pinus \text{ oocarpa} \quad (\text{B})$$

3.2. Vibration modes

A specimen may vibrate in different ways and for each mode there is a specific fundamental frequency. Figure 4 presents the main fundamental vibration modes [9].

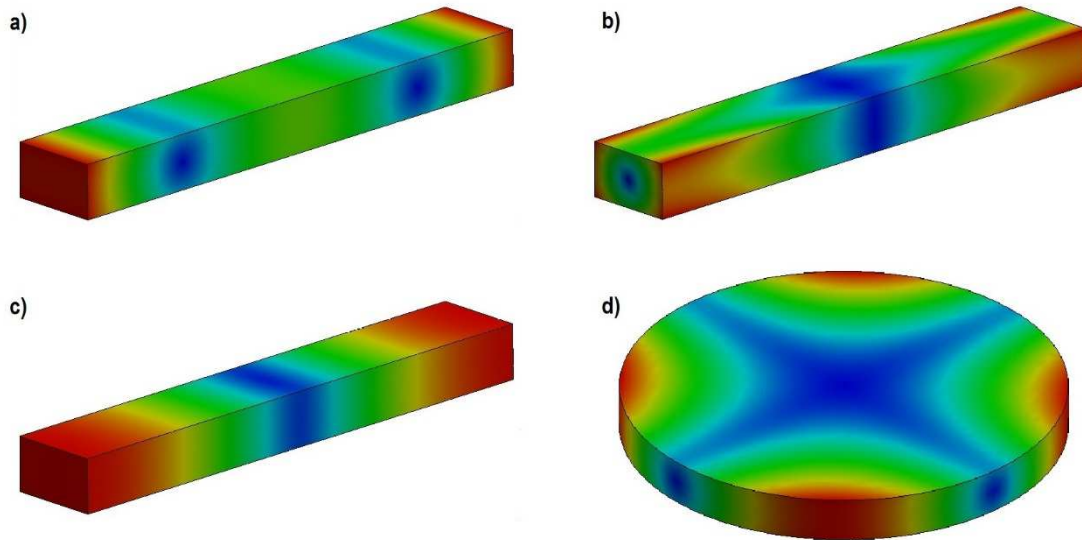


Figure 4 - Fundamental vibration modes: a) flexural, b) torsional, c) longitudinal, and e) planar. The blue region represents the area of minimum amplitude of vibration, whereas the red one represents the area of maximum amplitude.

Boundary conditions imposed during characterization are responsible for determining which vibration mode will be excited. The fundamental frequencies of these modes are affected by the geometry, mass, dimensions and elastic moduli.

Figures 5 a-c [1,6] present the optimum boundary conditions for the main vibration modes of a bar, whereas Figure 5d presents the optimum boundary conditions for a disc. The corresponding dynamic elastic moduli are calculated based on the resonant frequencies (determined by the vibration mode excited), and by employing the equations described in ASTM E1876 [1].

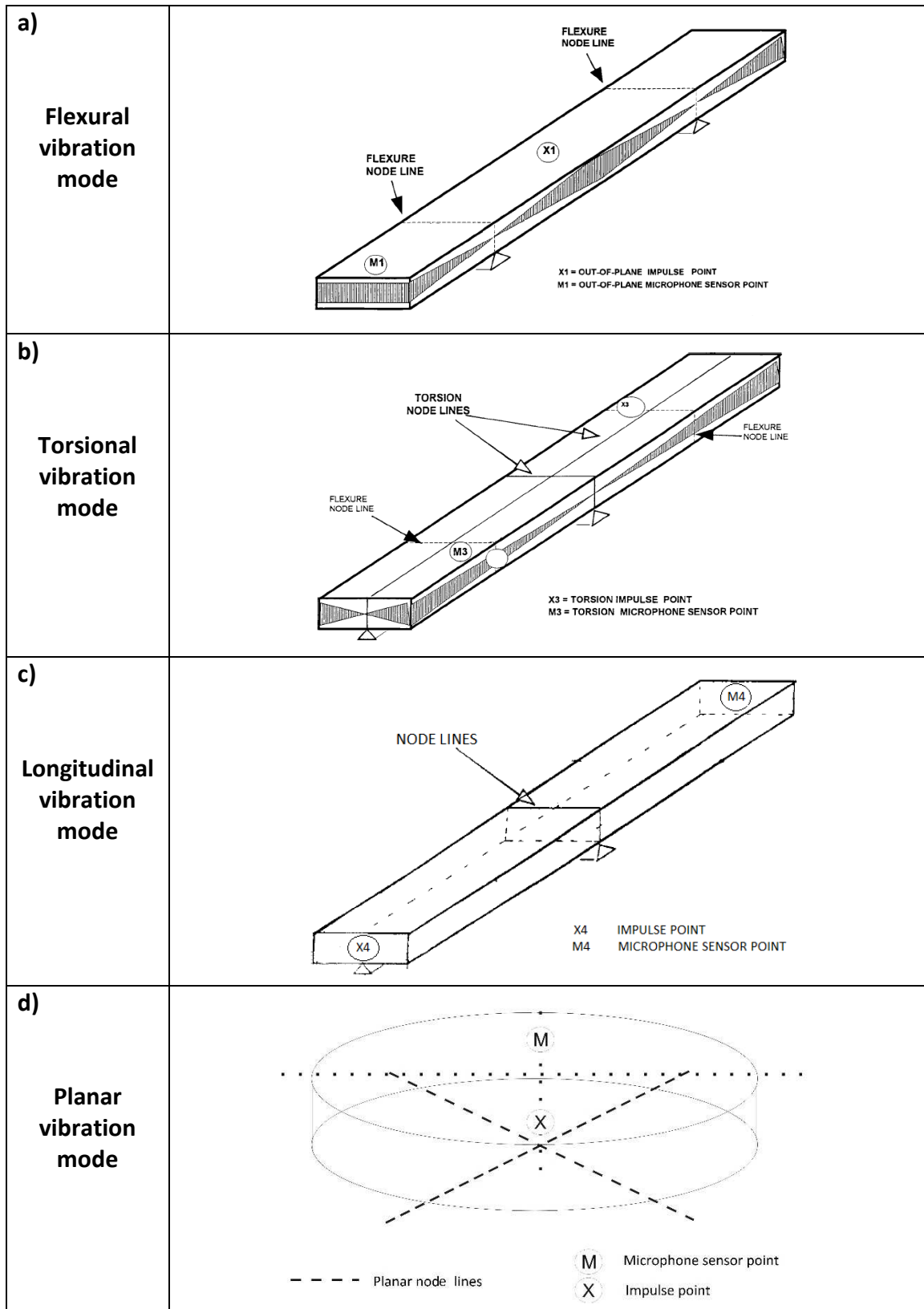


Figure 5 - Boundary conditions for the excitation of (a) flexural, (b) torsional, (c) longitudinal, and (d) planar fundamental vibration modes.

3.3. Elastic moduli of wood specimens

Wood specimens present a varied range of properties depending on the orientation of its fibers (grain direction) and growth rings. When they are characterized using the Impulse Excitation Technique, it is important to consider these orientations and report which of the elastic moduli is being measured.

Table 1 - Elastic moduli measured according to the orientation of the sample and the vibration mode.

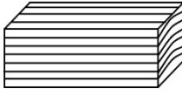
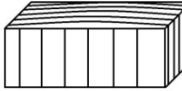
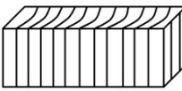
		Sample's orientation		
		Longitudinal	Tangential	Radial
				
Vibration mode	Flexural	E_L	E_T	E_R
	Torsional	$G_{eff} (G_{LT}, G_{LR})$	$G_{eff} (G_{LT}, G_{RT})$	$G_{eff} (G_{LR}, G_{RT})$
	Longitudinal	E_L	E_T	E_R

Table 1 indicates the elastic moduli that is characterized through the Impulse Excitation Technique in accordance to the vibration mode and sample's orientation. The terms used in Table 1 can be described as [5,10]:

E_L – Longitudinal Young's modulus;

E_T – Tangential Young's modulus;

E_R – Radial Young's modulus;

G_{eff} – Shear modulus (modulus of rigidity) characterized by the Sonelastic® equipment.

It corresponds to a combination of the G_{ij} moduli shown in parentheses [5];

G_{LT} – Modulus of Rigidity associated to shear strain at the LT plane resulting from shear stresses in the LR and RT planes;

G_{RT} – Modulus of Rigidity associated to shear strain at the RT plane resulting from shear stresses in the LR and LT planes;

G_{LR} – Modulus of Rigidity associated to shear strain at the LR plane resulting from shear stresses in the RT and LT planes.

3.3.1 Young's modulus

- **Longitudinal vibration mode**

When the sample is excited in longitudinal mode (check boundary conditions in Figure 5c), the elastic modulus obtained will refer to the orientation parallel to the sample's length. Therefore, the orientation of the sample will determine the elastic modulus being measured (E_1 , E_2 , E_3 or a combination of these directions), as presented in Table 1.

- **Flexural vibration mode**

When a sample is flexed, there are both tension and compression present, as pictured in Figure 6. For homogeneous and isotropic materials, the elastic modulus obtained from a bending test coincides with the elastic modulus measured in an axial test (longitudinal direction). Therefore, the value of a dynamic elastic modulus obtained through the flexural vibration mode is the same as the one obtained through the longitudinal vibration mode [11]. Nevertheless, it is known that when flexed, the surface is the region submitted to the greatest values of normal stress. For this reason, if a sample presents the stiffness of the surface different from the inside (for example, if there is a stiffness gradient along the thickness), or if the sample presents small flaws such as pores, cracks and micro-cracks on the surface, there will be a difference between the values obtained through flexural and longitudinal vibration modes. In the literature, there is a range of publications focused on the wood evaluation, presenting the difference between values obtained from distinct vibration modes [10, 12-14].

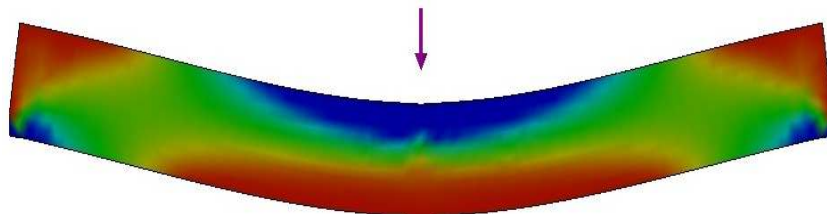


Figure 6 - Regions of tension (red) and compression (blue) stress during a bending test.

3.3.2 Shear modulus (modulus of rigidity)

- **Torsional vibration mode**

When a sample is submitted to a torsion test, two values of shear modulus act concomitantly on the material. If there is torsion such as described in Figure 5b, the acting modulus of rigidity are associated with the surfaces that are being sheared (the four laterals of the sample), for this reason, the shear modulus calculated using fundamental torsional frequency will correspond to an effective modulus. In other words, the result obtained by the Sonelastic® will be a combination of the active shear moduli (Table 1 indicates the active shear moduli that comprise the effective value for each orientation) [5].

3.3.3 Poisson's ratio

The Impulse Excitation Technique is not suitable to characterize the Poisson's ratio of orthotropic materials such as wood. However, based on the Elasticity Theory (using the stiffness matrix) it is possible to obtain correlations between the Poisson's ratio and the Young's modulus. Next, find the description of such relations (in Appendix A is possible to visualize the stiffness matrix for these materials):

$$\frac{\nu_{LR}}{E_L} = \frac{\nu_{RL}}{E_R}, \quad \frac{\nu_{LT}}{E_L} = \frac{\nu_{TL}}{E_T}, \quad \frac{\nu_{RT}}{E_R} = \frac{\nu_{TR}}{E_T}$$

3.4. Expected values for the elastic moduli of wood

Wood may be classified as softwood or hardwood. In general, hardwood presents higher elastic moduli and strength values [2].

Table 2 presents predicted elastic moduli values as a function of E_L for softwood, showing the elastic properties of this type of wood according to the E_L variation.

Table 2 – Predicted elastic parameters as function of E_L for softwood (values in GPa) [5]

E_L	E_R	E_T	G_{LR}	G_{LT}	G_{RT}
6.0	0.6990	0.3667	0.6564	0.6185	0.0518
7.0	0.7710	0.4069	0.6763	0.6366	0.0566
8.0	0.7856	0.4453	0.6962	0.6546	0.0612
9.0	0.8241	0.4821	0.7161	0.6727	0.0655
10.0	0.8601	0.5177	0.7353	0.6907	0.0696
11.0	0.8940	0.5521	0.7558	0.7088	0.0736
12.0	0.9262	0.5855	0.7756	0.7268	0.0774
13.0	0.9567	0.6180	0.7955	0.7449	0.0811
14.0	0.9860	0.6497	0.8154	0.7629	0.0846
15.0	1.0140	0.6806	0.8352	0.7810	0.0881
16.0	1.0409	0.7109	0.8551	0.7990	0.0914
17.0	1.0668	0.7406	0.8750	0.8170	0.0946
18.0	1.0919	0.7698	0.8948	0.8351	0.0979

4. Case Study #1: Characterization of Eucalyptus bars using Sonelastic® solutions

This case study describes the characterization of prismatic bars of Eucalyptus (*Eucalyptus sp.*) with two distinct orientations using Sonelastic® solutions (Impulse Excitation Technique).

4.1. Materials and methods

Figure 7 shows a top view of a tree section, the concentric circles correspond to its growth rings. In this figure, three possible sample cuts are illustrated. The samples indicated by (1) and (2) present ideal cuts to obtain values for E_T and E_R , respectively. In (1), the length direction is tangent to the growth rings and in (2), the length direction is parallel to the direction of the growth rings [5].

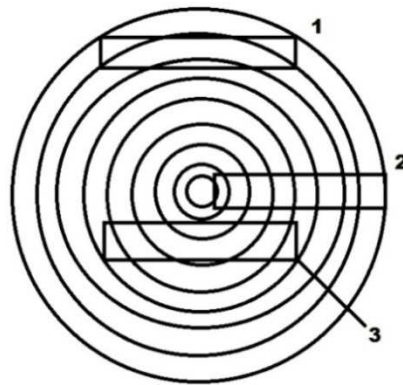


Figure 7 - Identification of the best places to cut the wood samples in order to characterize E_T (1) and E_R (2). The cut presented in (3) combines both R and T directions.

On the other hand, the sample indicated in (3) combines both R and T directions. As presented in this case study, it is possible to characterize samples with this orientation, however the values obtained will be effective, being a combination between E_R and E_T .

Figures 8 and 9 indicate the fibers orientation of the characterized wood samples. It is possible to see that the sample illustrated in Figure 8 presents the fibers aligned parallel to its length (these bars were indicated by “L” index). On the other hand, it is possible to see that the sample illustrated in Figure 9 has its fibers transversely oriented and there is a combination between the radial and tangential direction along its length (these bars were indicated by “RT” index).



Figure 8 - Sample presenting fibers aligned parallel to its length.



Figure 9 - Sample presenting combined radial and tangential orientation parallel to its length.

The dimensions of the samples were 145 mm x 25 mm x 25 mm and they were measured by a caliper rule. The mass was measured by using an analytical balance. These parameters are necessary for the elastic moduli calculation according to ASTM E1876.

The Sonelastic[®] equipment was employed in order to carry out the characterization via Impulse Excitation Technique.

The samples were characterized regarding the main vibration modes (flexural, torsional and longitudinal) using the SA-BC adjustable support for bars and cylinders, the IED Automatic Electromagnetic Impulse Device, the CA-DP High directional acoustic sensor, and the *Sonelastic software* (these items are part of the Sonelastic[®] solutions for the characterization of medium-sized samples). Figure 10 presents the equipment set up as previously described.

A Poisson's ratio of 0.25 ± 0.25 was adopted to calculate the elastic moduli. As mentioned earlier, this value may vary significantly according to the orientation of the fibers. For this reason, an uncertainty of 0.25 was considered, including all the possible

values for this property (PS: the influence of the Poisson's ratio when calculating the elastic moduli is low. This can be verified by checking the errors presented in Tables 5 and 6).



Figure 10 - Sonelastic® equipment developed by ATCP Physical Engineering for elastic moduli characterization via Impulse Excitation Technique.

4.2. Results and discussions

The samples were divided into two main groups using the direction of fibers as division criteria. Tables 3 and 4 show the dimensions and mass values for the samples. Tables 5 and 6 show the elastic moduli values obtained by using the Sonelastic® equipment.

Table 3 – Dimensions and mass of “RT” samples.

Sample	Length, L (mm)	Width, W (mm)	Thickness, T (mm)	Mass (g)
RT – 01	142.95 ± 0.15	24.05 ± 0.15	24.35 ± 0.15	77.44 ± 0.01
RT – 02	144.95 ± 0.15	24.15 ± 0.15	24.35 ± 0.15	77.37 ± 0.01
RT – 03	143.80 ± 0.15	23.90 ± 0.15	24.00 ± 0.15	78.01 ± 0.01
RT – 04	143.20 ± 0.15	24.20 ± 0.15	24.35 ± 0.15	68.73 ± 0.01

Table 4 - Dimensions and mass of “L” samples.

Sample	Length, L (mm)	Width, W (mm)	Thickness, T (mm)	Mass (g)
L – 01	144.05 ± 0.15	24.10 ± 0.15	23.95 ± 0.15	63.65 ± 0.01
L – 02	144.25 ± 0.15	23.95 ± 0.15	24.10 ± 0.15	76.74 ± 0.01
L – 03	143.90 ± 0.15	23.60 ± 0.15	23.85 ± 0.15	75.22 ± 0.01
L – 04	144.00 ± 0.15	24.25 ± 0.15	24.40 ± 0.15	64.34 ± 0.01

Table 5 - Elastic moduli values obtained as a function of the vibration mode (“RT” samples).

Samples	Longitudinal mode	Flexural mode	Torsional mode
	E_{eff} (GPa)	E_{eff} (GPa)	G_{eff} (GPa)
RT – 01	1.45 ± 0.05	1.50 ± 0.06	1.20 ± 0.01
RT – 02	1.23 ± 0.04	1.30 ± 0.05	1.12 ± 0.01
RT – 03	1.55 ± 0.05	1.67 ± 0.06	1.25 ± 0.01
RT – 04	1.40 ± 0.05	1.45 ± 0.05	1.21 ± 0.01
Average value	1.41	1.48	1.20
Standard deviation	0.13	0.15	0.05

Table 6 - Elastic moduli values obtained as a function of the vibration mode (“L” samples).

Sample	Longitudinal mode	Flexural mode	Torsional mode
	E_L (GPa)	E_L (GPa)	G_{eff} (GPa)
L – 01	18.01 ± 0.64	13.16 ± 0.49	1.13 ± 0.01
L – 02	22.39 ± 0.79	17.87 ± 0.66	1.34 ± 0.01
L – 03	21.33 ± 0.76	17.23 ± 0.64	1.43 ± 0.02
L – 04	18.19 ± 0.64	14.19 ± 1.15	1.15 ± 0.01
Average value	19.98	15.61	1.26
Standard deviation	2.21	2.29	0.15

The Young’s modulus values indicated in Table 5 are effective because the samples present a combination between R and T directions aligned parallel to their lengths. The values measured for “L” samples are represented by E_L because the fibers are parallel to the length (Table 6).

There is a difference observed between elastic moduli values obtained in longitudinal and flexural directions, mainly for the “L” samples. Such difference may be explained by two main factors: the first and most critical is the presence of defects, such as small cracks on the sample’s surface, negatively influencing measurements taken from flexural tests. Another factor that may influence the measurement is the presence of a stiffness gradient along the sample’s thickness, which may alter the values obtained. For wood specimens, there is a tendency of properties based on the longitudinal mode being superior to the ones obtained from flexural mode [10,12-14].

Finally, G_{eff} consists of a modulus of rigidity, which is a combination of the moduli related to the planes that are being sheared on the torsional vibration. For example, the G_{eff} value for the “L” samples is a combination between G_{LR} and G_{LT} . On the other hand, for the “RT” samples, this analysis is more complex because the direction of the sample’s length does not correspond to a defined orientation (L, R or T).

5. Case study #2: Estimation and characterization of the Young's modulus of a cylindrical metallic composite and of a wooden log with heartwood and sapwood

This case study presents a model to predict the Young's modulus of two cylinders concentrically arranged on the same sample, using as input parameters the longitudinal (E_{long}) and flexural (E_{flex}) elastic moduli of the cylinder composite. In addition, this model was also used to predict the Young's modulus of heartwood and sapwood from a wooden log based on the characterization of a sample containing these elements.

One of the goals of this work was to investigate in details the reason why the Young's modulus value of wood and wood products obtained by the longitudinal vibration mode was different from the one obtained by the flexural mode. In addition, it also aimed to construct a model capable to predict simultaneously and non-destructively the Young's modulus of a cylindrical sample made from two components.

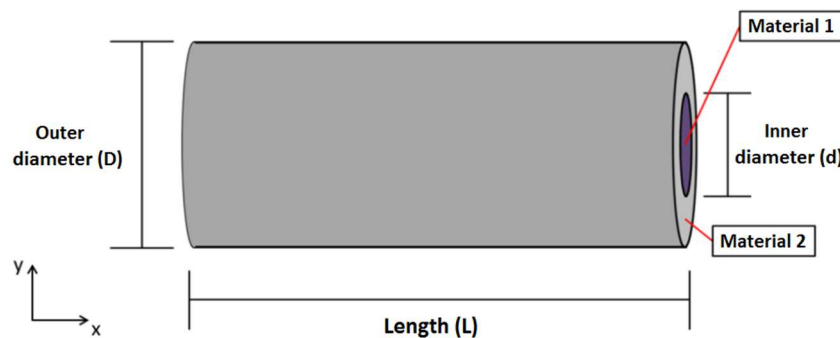


Figure 11 - Diagram of a cylindrical composite such as the one used in this study.

5.1. Fundamentals and equations

The variance in stiffness along the thickness of a sample is one of the main reasons that explain the different values of Young's modulus obtained through flexural and uniaxial tests for the same specimen. This difference may occur in two special occasions. The first depends on the amount of defects found on the surface of the specimen, such as cracks and micro-cracks (in this case, the values obtained from a flexural test tend to differ from those from a tensile test). The second occurs when there is a stiffness gradient along the sample's thickness (the stress distribution in a bending test is not uniform along the transversal section and the external areas, which will be

submitted to higher values of stress, will be the ones influencing the most the obtained values).

Different types of wood, because of their chemical composition and anatomical disposition, tend to be more rigid under tension than under compression (in experiments parallel to the direction of the fibers). The influence of such distinct behaviors may affect differently the longitudinal and flexural vibration modes, presenting different values of stiffness depending on the excitation form.

For this reason, different approaches should be used to predict the Young's modulus of a cylindrical composite. If the sample does not present superficial cracks on its surface, it is possible to predict simultaneously and non-destructively the Young's modulus values of its components. Below are presented the final equations used in the predictions (the complete development of the models is described in Appendix B).

$$E_1 = \frac{E_{long}(D^2 + d^2) - E_{flex}D^2}{d^2} \quad (C)$$

$$E_2 = \frac{E_{flex}D^2 - E_{long}d^2}{(D^2 - d^2)} \quad (D)$$

E_1 represents the Young's modulus of the inner material of the cylinder (heartwood region, for example); E_2 , the Young's modulus of the outer material (sapwood region, for example); D , the outer diameter of the cylinder; and d , the inner diameter of the cylinder (see diagram in Figure 11).

5.2. Materials and methods

The materials used in the initial tests were a steel cylinder ($\rho_{ap} = 7.8 \text{ g/cm}^3$) of 11.75 mm of diameter, and an aluminum cylinder ($\rho_{ap} = 2.8 \text{ g/cm}^3$) of 29.71 mm of diameter, both solid cylinders. To evaluate the elastic moduli of a wooden specimen, a lathed wooden log composed of heartwood and sapwood was used, as well as two rectangular bars of the heartwood and the sapwood separately.

A hole of approximately 12.0 mm of diameter was made on the center of the transversal section of the aluminum cylinder, so that the solid steel cylinder could fit in its interior. Then, an epoxy glue was used to fix the steel cylinder in the interior of the

aluminum sample. Figure 12 shows a diagram representing the cylindrical metallic composite ($\rho_{ap} = 3,6 \text{ g/cm}^3$) used in the preliminary studies.

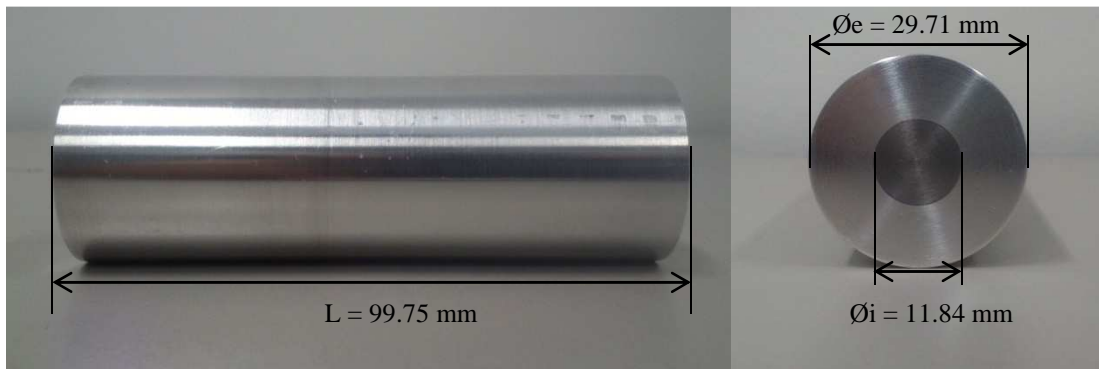


Figure 12 – Cylindrical metallic composite (outer material: aluminum; inner material: steel).

After applying the equations to the metallic cylinder, the model was also used to predict the Young's modulus of the wooden cylinder. To compare the findings and also verify if the model was valid for the wood, both heartwood and sapwood samples were separately characterized. Figure 13 illustrates the wooden cylinder used and Figure 14, the heartwood and sapwood samples.



Figure 13 – Lathed wooden log with a good superficial finishing, highlighting the central region of the log composed by heartwood, and the external region, composed by sapwood.

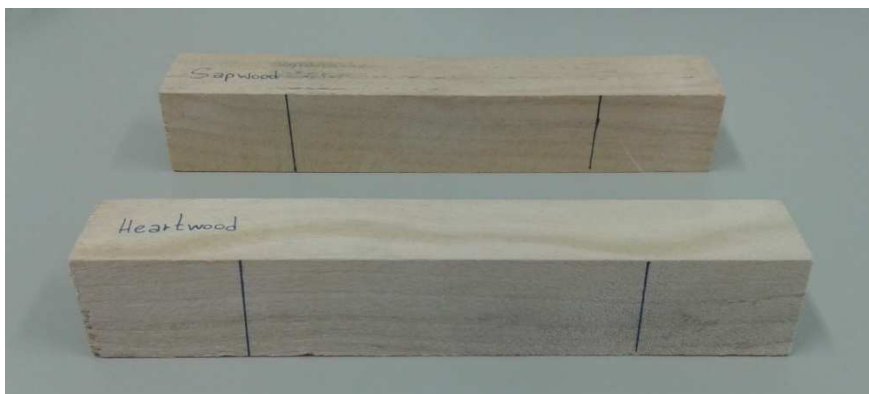


Figure 14 – Heartwood and sapwood samples.

5.3. Results and discussions

5.3.1. Metallic composite

Table 7 shows the dimensions and mass values of the metallic parts. The results obtained using Sonelastic[®] are presented in Table 8.

Table 7 - Mass and dimensions of metallic cylindrical samples.

	Mass (g)	L (mm)	Deviation	D (mm)	Deviation	d (mm)
Solid aluminum	194.56	99.94	0.03	29.71	0.03	-
Steel	118.61	139.65	0.05	11.75	0.09	-
Cylindrical composite	246.76	99.75	0.04	29.71	0.04	11.84

Table 8 – Elastic moduli values for the metallic cylinders (obtained by Sonelastic[®] solutions).

	E_{flex} (GPa)	Uncertainty	E_{long} (GPa)	Uncertainty
Solid aluminum (material 1)	72.19	0.54	71.88	0.45
Steel (material 2)	211.84	7.60	213.01	3.96
Cylindrical composite	77.38	0.67	93.34	0.61

Therefore, when applying the prediction models to calculate the Young's modulus of steel and aluminum:

$$E_1 = E_{steel} = \frac{93.34 \times (29.71^2 + 11.84^2) - 77.38 \times 29.71^2}{11.84^2} = 193.83 \text{ GPa}$$

$$E_2 = E_{aluminum} = \frac{77.38 \times 29.71^2 - 93.34 \times 11.84^2}{(29.71^2 - 11.84^2)} = 74.37 \text{ GPa}$$

Table 9 shows the elastic moduli predicted by the model and the elastic moduli obtained experimentally by the Sonelastic[®] equipment.

Table 9 – Comparison between the theoretical model and the experimental values of the metallic cylinders.

	E_{steel} (GPa)	E_{alum} (GPa)
Theoretical (predicted by the model)	193.83	74.37
Experimental (Sonelastic [®])	211.84	72.19
Absolute variation*	18.01	2.18
Variation (%)*	8.5%	3.0%

* Absolute variation (VA) = |Exp. – Theoretical| and Variation (%) = (VA/Exp.)*100

It is noticeable the fact that there was a slight variation between the measured and predicted values. The main causes of these differences are: the model considered that the isolated materials presented $E_{flex} = E_{long}$ (which was not visualized when separately characterizing them); it was disregarded the effect of the thin layer of the epoxy glue; and, finally, the influence of Poisson's ratio was not considered.

Nevertheless, it is possible to affirm that there was a good agreement between the model and the characterizations made by the Sonelastic[®] equipment.

5.3.2. Wooden samples

Tables 10 and 11 show the dimensions and mass values regarding the wooden cylinder and the prismatic heartwood and sapwood bars, respectively.

Table 10 – Mass and dimensions of the wooden cylinder.

	Mass (g)	L (mm)	Deviation	Øo (mm)	Deviation	Øi (mm)
Cylinder	1849.91	408.33	1.25	88.47	0.50	58.40

Table 11 – Mass and dimensions of heartwood and sapwood samples.

	Mass (g)	L (mm)	Deviation	W (mm)	Deviation	H (mm)	Deviation
Sapwood 1	89.85	151.57	0.36	25.60	0.09	25.79	0.08
Sapwood 2	90.31	151.84	0.09	25.14	0.16	25.64	0.18
Heartwood 1	61.65	151.86	0.13	25.63	0.17	24.53	0.25
Heartwood 2	62.83	151.73	0.06	25.66	0.09	25.03	0.22

The results obtained for the wooden cylinder are shown in Table 12, whilst the results for heartwood and sapwood samples are in Table 13.

Table 12 - Results for the wooden cylinder (obtained by Sonelastic[®] solutions).

	E_{flex} (GPa)	Uncertainty	E_{long} (GPa)	Uncertainty
Wooden cylinder	7.93	0.24	8.84	0.16

Table 13 - Results for the heartwood and sapwood samples (obtained by Sonelastic[®] solutions).

	E_{flex} (GPa)	Uncertainty	E_{long} (GPa)	Uncertainty
Sapwood 1	8.80	0.16	10.03	0.16
Sapwood 2	7.90	0.22	8.42	0.21
Heartwood 1	7.95	0.30	9.23	0.28
Heartwood 2	8.43	0.28	10.04	0.25

By looking at table 13, it is possible to visualize that the Young's modulus of heartwood and sapwood samples was nearly the same, if considering the measurement uncertainties. The observed difference between the longitudinal and flexural values for the wooden cylinder can be attributed to the integrity of its surface, that despite being lathed, presented some small cracks (affecting negatively the results obtained by flexural tests).

The possible explanation of the difference in stiffness between heartwood and sapwood mainly involves the age of the formed tissue and the quantity of defects presented. However, because of the natural character of these materials, other parameters may be pointed as possible contributors for the increase or decrease in elastic modulus of these specific regions [15].

For the case of the wood sample evaluated herein, it is possible to visualize that the influence of the superficial integrity overlapped the influence of the stiffness difference between the sapwood and the heartwood for this species of wood (as presented, the elastic moduli of these two areas were almost the same).

6. Final considerations

Wood presents anisotropic characteristics, meaning that its properties are dependent on the orientation from which the measurements are being taken. For this reason, the main direction of the sample must always be considered and referenced in the results of the evaluated property.

Based on the wooden sample's orientation and by applying the correct boundary conditions for flexural and longitudinal modes, it is possible to obtain the three main elastic moduli: E_L , E_R and E_T . The Impulse Excitation Technique also allows the characterization of an effective modulus of rigidity by exciting a sample in the torsional vibration mode.

Lastly, it was presented a case study and a model to predict simultaneously and non-destructively the heartwood and sapwood Young's modulus values through the Impulse Excitation Technique (Sonelastic®) based on the longitudinal and flexural vibration tests of a wooden cylinder. The study herein also showed that the integrity of the surface will also significantly affect the measurements, and may be the main reason to explain the different values of elastic moduli obtained through flexural and longitudinal vibration tests.

7. References

- [1] ASTM International. *Standard Test Method for Dynamic Young's Modulus, Shear Modulus, and Poisson's Ratio by Impulse Excitation of Vibration*; ASTM E 1876. 2007. 15 p.
- [2] DİNÇKAL, Ç. Analysis of Elastic Anisotropy of Wood Material for Engineering Applications. *Journal of Innovative Research in Engineering and Science*, Global Research Publishing, pp. 67-80, April 2011.
- [3] Wood bridge in Montmorency forest. Available at:
<http://upload.wikimedia.org/wikipedia/commons/b/be/Wood_bridge_Montmorency.jpg>. Accessed on: 18th of March, 2013.
- [4] Adapted from CALIL JUNIOR, C.; LAHR, F.A.R.; DIAS, A.A. *Dimensionamento de elementos estruturais de madeira*. Barueri: Manole, 2003. 152 p.
- [5] BODIG, J., JAYNE, B. A. *Mechanics of wood and wood composites*. Malabar (EUA), Krieger Publishing Company, 1993.
- [6] COSSOLINO, L.C., PEREIRA, A.H.A. Módulos elásticos: visão geral e métodos de caracterização. Informativo Técnico – ATCP Engenharia Física. Out/2010. Available at: <<http://www.atcp.com.br/imagens/produtos/sonelastic/artigos/RT03-ATCP.pdf>>. Accessed on: 18th of March, 2013.
- [7] SEGUNDINHO, P.G.A., COSSOLINO, L.C., PEREIRA, A.H.A, JUNIOR, C.C. Aplicação do método de ensaio das frequências naturais de vibração para obtenção do módulo de elasticidade de peças estruturais de madeira. *Revista Árvore*, Viçosa-MG, v.36, n.6, p.1155-1161, 2012.
- [8] Positioning and characterization scheme in accordance to ASTM E1876. Adapted from: <<http://www.atcp.com.br/pt/produtos/caracterizacao-materiais/propriedades-materiais/modulos-elasticos/metodos-caracterizacao-.html>> Accessed on: 4th of April, 2013.
- [9] HEYLIGER, P., UGANDER, P., LEDBETTER, H. Anisotropic Elastic Constants: Measurement by Impact Resonance. *Journal of Materials in Civil Engineering*, pp. 356-363, Sep/Oct 2001.
- [10] WANGAARD, F.F. *The Mechanical Properties of Wood*. New York: John Wiley & Sons, Inc, 1950.
- [11] KAW, A.K. *Mechanics of composite materials*. Boca Raton: Taylor & Francis Group, 2 ed, 2006, 457 p.
- [12] ROCHA, J.S., PAULA, E.V.C.M. de, SIQUEIRA, M.L. Flexão Estática em amostras pequenas livres de defeitos. *Acta Amazonica*, Manaus, p. 147-162. 1988.
- [13] CHO, C.L., Comparison of Three Methods for Determining Young's Modulus of Wood. *Taiwan Journal for Science*, pp. 297-306, May/2007.
- [14] BUCUR, V., *Acoustics of Wood*. 2^a ed. Germany: Springer, 2006. p. 393.
- [15] WANGAARD, F. F. *The Mechanical Properties of Wood*. John Wiley & Sons, Inc., New York, 1950.
- [16] CALLISTER Jr., W.D. *Materials Science and Engineering*. 7^a ed. New York: John Wiley & Sons, Inc, 2007.
- [17] Stress-strain curve. Adapted from:
<http://www.ctb.com.pt/?page_id=1471>. Accessed on: 8th of July, 2014.
- [18] NYE, J.F. *Physical Properties of Crystals: their representation by tensors and matrices*. Oxford: At the Clarendon Press. 1957.

Appendix A – Elasticity theory applied to wood

Wood is an anisotropic material, therefore its properties vary according to the direction of the load. For this reason, the Elasticity Theory, when applied to this type of material, is much more complex than when it is applied to isotropic materials. Thus, considering the complexity of the material under study, this appendix includes the correct way in which the elastic properties should be presented and defined.

- **Introduction: Young’s modulus – Hooke’s law**

Based on a tensile test of an isotropic material (an annealed metal, for example), at the elastic regime, it is possible to correlate stress and strain as described by Equation 1 (Hooke’s law) [16]:

$$\sigma = E \cdot \varepsilon \quad (1)$$

Figure 15 shows a typical stress-strain curve of a quasi-static tensile test from which the main mechanical properties are obtained. The Young’s modulus, E , is the slope of the curve when the sample is under the elastic regime (beginning of the curve).

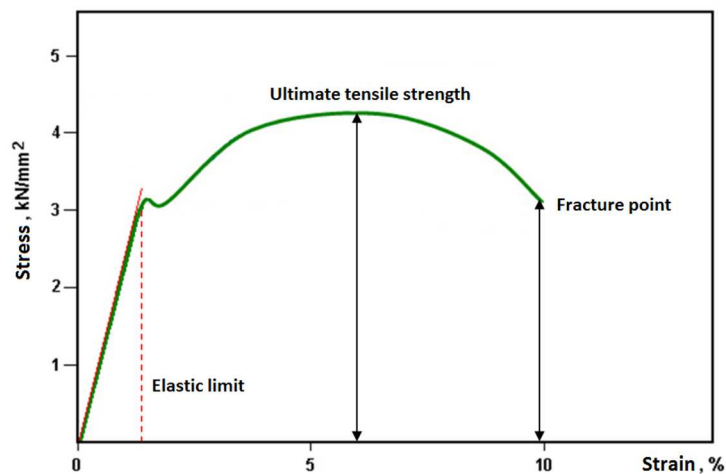
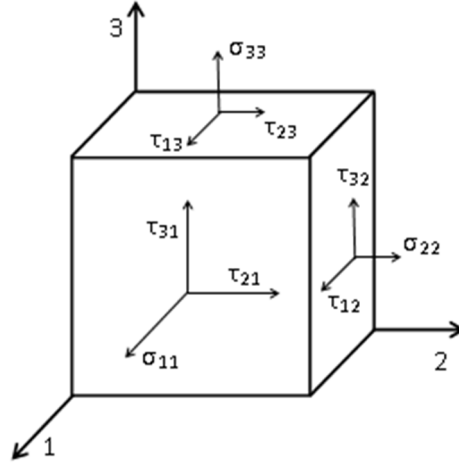


Figure 15 – Stress-strain curve of a high-strength steel [17].

- **Stress and strain – tridimensional model**

The diagram below presents an infinitesimal volume with possible stress types that may appear whilst loading a sample.



Note that there are two stress types present in this model: the tensile stress represented by σ , and the shear stress, represented by τ . Taking that into consideration, this model may be represented by a 3 x 3 matrix (Equation 2):

$$[\sigma_{ij}] = \begin{bmatrix} \sigma_{11} & \tau_{12} & \tau_{13} \\ \tau_{21} & \sigma_{22} & \tau_{23} \\ \tau_{31} & \tau_{32} & \sigma_{33} \end{bmatrix} \quad (2)$$

Assuming that there is a balance of forces within this volume, shear stresses oriented to the same edge of the cube are equivalent (for instance, $\tau_{12} = \tau_{21}$). Therefore, the load applied can be represented by six distinct stresses, as shown in the symmetric matrix below:

$$[\sigma_{ij}] = \begin{bmatrix} \sigma_{11} & \tau_{12} & \tau_{13} \\ & \sigma_{22} & \tau_{23} \\ & & \sigma_{33} \end{bmatrix} \quad (3)$$

The same analysis can be made regarding the strain:

$$[\varepsilon_{ij}] = \begin{bmatrix} \varepsilon_{11} & \frac{1}{2}\gamma_{12} & \frac{1}{2}\gamma_{13} \\ & \varepsilon_{22} & \frac{1}{2}\gamma_{23} \\ & & \varepsilon_{33} \end{bmatrix} \quad (4)$$

- **Anisotropic elasticity**

As it was previously described, wood presents different behavior according to the load direction, consequently, the stress-strain correlations are not the same for all the directions. Therefore, it is always necessary to consider the orientation of the sample before characterizing its elastic properties.

The general Hooke's law is more complex because it considers the stress and strain matrices described in the previous item. It is given by the following correlation:

$$\sigma_{ij} = C_{ijkl} \cdot \varepsilon_{kl}, \quad \text{in which } i, j, k, l = 1, 2, 3 \quad (5)$$

Considering the stress and the strain as square matrices of third order, it is possible to conclude that C_{ijkl} is a fourth-order tensor, known as stiffness tensor [11]. Based on the relationships of symmetry described below, it is possible to lower the number of elastic constants from 81 to 21.

$$C_{ijkl} = C_{jikl}, \quad C_{ijkl} = C_{ijlk}, \quad C_{ijkl} = C_{klij} \quad (6)$$

A reduced index notation is used to simplify the correlation between stress, strain and elastic constants, as shown in Table 14.

Table 14 - A four-index notation reduced to a two-index notation [18].

Four-index notation	11	22	33	23	31	12
Two-index notation	1	2	3	4	5	6

Based on all previous considerations, the stiffness matrix of an anisotropic material presenting linear-elastic behavior is symmetric and may be described as:

$$\begin{bmatrix} \sigma_1 \\ \sigma_2 \\ \sigma_3 \\ \tau_4 \\ \tau_5 \\ \tau_6 \end{bmatrix} = \begin{bmatrix} C_{11} & C_{12} & C_{13} & C_{14} & C_{15} & C_{16} \\ & C_{22} & C_{23} & C_{24} & C_{25} & C_{26} \\ & & C_{33} & C_{34} & C_{35} & C_{36} \\ & & & C_{44} & C_{45} & C_{46} \\ & & & & C_{55} & C_{56} \\ & & & & & C_{66} \end{bmatrix} \cdot \begin{bmatrix} \varepsilon_1 \\ \varepsilon_2 \\ \varepsilon_3 \\ \gamma_4 \\ \gamma_5 \\ \gamma_6 \end{bmatrix} \quad (7)$$

Another form to represent the stress-strain relation of a material is by using the compliance matrix, as shown in Equation 8:

$$\begin{bmatrix} \varepsilon_1 \\ \varepsilon_2 \\ \varepsilon_3 \\ \gamma_4 \\ \gamma_5 \\ \gamma_6 \end{bmatrix} = \begin{bmatrix} S_{11} & S_{12} & S_{13} & S_{14} & S_{15} & S_{16} \\ & S_{22} & S_{23} & S_{24} & S_{25} & S_{26} \\ & & S_{33} & S_{34} & S_{35} & S_{36} \\ & & & S_{44} & S_{45} & S_{46} \\ & & & & S_{55} & S_{56} \\ & & & & & S_{66} \end{bmatrix} \cdot \begin{bmatrix} \sigma_1 \\ \sigma_2 \\ \sigma_3 \\ \tau_4 \\ \tau_5 \\ \tau_6 \end{bmatrix} \quad (8)$$

i.e.,

$$[S] = [C]^{-1} \quad (9)$$

It is possible to note that to fully describe a material regarding the elastic properties, it is necessary to find its 21 elastic constants. It is also important to highlight that this model represents the elastic properties measured from a specific point of a material, meaning that the described constants may vary from point to point if the material is not homogeneous. Despite the fact that wood is a heterogeneous material, to simplify the model, it is common to consider wood as being homogeneous.

- **Types of material and present symmetries**

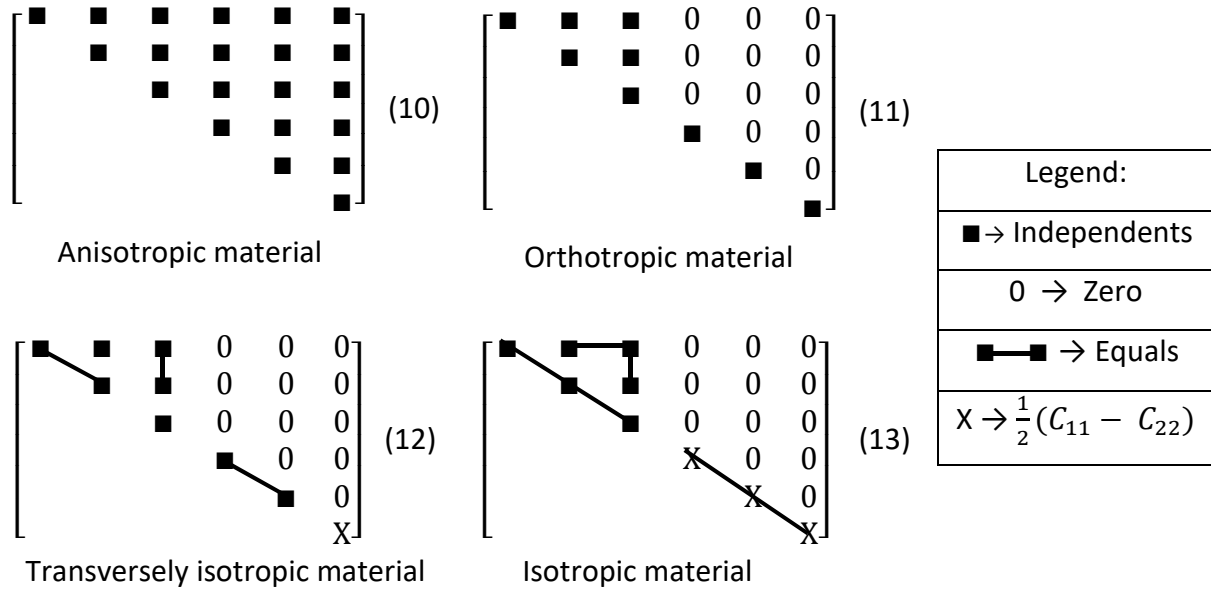
Despite the variation in properties depending on the load direction, most materials present an internal organization, making possible to simplify the elastic matrix parameters presented in the previous item.

A material that does not present a plane of symmetry is called “anisotropic”, and all of its elastic constants are independent from each other [5].

If a material varies its properties depending on the load direction, but has orthogonal planes of symmetry, they are called “orthotropic materials”. Wood is generally classified as such. To be able to fully characterize a sample presenting this type of symmetry, it is necessary to obtain nine independent variables [5].

If a material with an orthogonal symmetry has one of its planes isotropic, it can be classified as being “transversely isotropic” (in the case of wood, this situation would occur if the tangential properties were the same as the radial properties).

Lastly, the simplest possible case that has the smallest number of independent variables is when the material presents isotropy in infinite planes. In that case, the material is called as being “isotropic”, meaning that the properties do not vary with the direction, and the stiffness matrix will depend only on two variables [5].



• **Elastic constants of wood**

According to the previous topic, wood is classified as being an orthotropic material and to fully characterize its elastic behavior, nine independent variables are needed. Next is presented the compliance matrix, described according to its elastic constants. Note that indexes 1, 2 and 3 have been replaced by wood specific indexes: L (longitudinal), R (radial) and T (tangential), respectively [5].

• Compliance matrix:

$$\begin{bmatrix} \varepsilon_L \\ \varepsilon_R \\ \varepsilon_T \\ \gamma_{RT} \\ \gamma_{LT} \\ \gamma_{LR} \end{bmatrix} = \begin{bmatrix} \frac{1}{E_L} & -\frac{\nu_{RL}}{E_R} & -\frac{\nu_{TL}}{E_T} & 0 & 0 & 0 \\ -\frac{\nu_{LR}}{E_L} & \frac{1}{E_R} & -\frac{\nu_{TR}}{E_T} & 0 & 0 & 0 \\ -\frac{\nu_{LT}}{E_L} & -\frac{\nu_{RT}}{E_R} & \frac{1}{E_T} & 0 & 0 & 0 \\ 0 & 0 & 0 & \frac{1}{G_{RT}} & 0 & 0 \\ 0 & 0 & 0 & 0 & \frac{1}{G_{LT}} & 0 \\ 0 & 0 & 0 & 0 & 0 & \frac{1}{G_{LR}} \end{bmatrix} \times \begin{bmatrix} \sigma_L \\ \sigma_R \\ \sigma_T \\ \tau_{RT} \\ \tau_{LT} \\ \tau_{LR} \end{bmatrix} \quad (14)$$

By using this matrix, it is possible to determine the strains as a function of applied stresses if the elements (elastic constants) are all known.

Appendix B – Developing a model to predict the Young's modulus values of heartwood and sapwood in wooden cylinder

To develop a model for the prediction of longitudinal and flexural Young's modulus, it was necessary to use a cylinder made up of two metals concentrically arranged, such as pictured in Figure 11, case study #2.

- Longitudinal load (rule of mixtures) [11]:

By applying a longitudinal force at the cylinder, the load is equally distributed throughout the transversal section of the sample, as such:

$$F_x = F_1 + F_2 \quad (15)$$

Knowing that the load applied corresponds to the stress multiplied by the area:

$$\sigma_x \cdot A_T = \sigma_1 \cdot A_1 + \sigma_2 \cdot A_2 \quad (16)$$

Through the stress-strain correlation, the following equation is formed:

$$E_{eff} \cdot \varepsilon_x \cdot A_T = E_1 \cdot \varepsilon_1 \cdot A_1 + E_2 \cdot \varepsilon_2 \cdot A_2 \quad (17)$$

Considering equal strains in the case of a uniaxial load:

$$E_{eff} = E_1 \cdot \frac{A_1}{A_T} + E_2 \cdot \frac{A_2}{A_T} \quad (18)$$

Thus, the relation between the moduli will follow the rule of mixtures, being described by:

$$E_{eff} = E_1 \cdot V_{eq1} + E_2 \cdot V_{eq2} \quad (19)$$

where:

$$V_{eq1} = \frac{V_1}{V_T} = \frac{L \frac{\pi d^2}{4}}{L \frac{\pi D^2}{4}} = \frac{d^2}{D^2} \quad \text{and} \quad V_{eq2} = \frac{V_2}{V_T} = \frac{L \frac{\pi(D^2-d^2)}{4}}{L \frac{\pi D^2}{4}} = \frac{(D^2-d^2)}{D^2} \quad (20,21)$$

Replacing the results of equations 20 and 21 in equation 19, it is possible to correlate the longitudinal Young's modulus of a cylindrical composite as a function of the diameters and of the Young's modulus of its components.

$$E_{long}^{eff} = \frac{E_1 \cdot d^2 + E_2 \cdot (D^2 - d^2)}{D^2} \quad (22)$$

- Flexural load (Euler-Bernoulli equation):

The Euler-Bernoulli equation used to describe the beam flexure can be written as:

$$\frac{d^2}{dx^2} \left(E \cdot I_z \cdot \frac{d^2 w}{dx^2} \right) = -p \quad (23)$$

In which w is the displacement of the beam from the neutral line (see Figure 18); E is the Young's modulus of the material; I_z is the second moment of area and p is the linear density of load applied on the sample's surface.

The development to reach the Euler-Bernoulli equation (equation 23) is described below. However, it was focused on the study of a beam formed by two distinct materials.

Initially, equilibrium equations are applied to an infinitesimal element of a rectangular bar through a bending test, such as described in Figure 16.

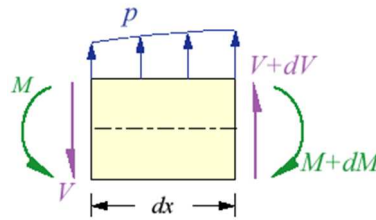


Figure 16 - Forces and resulting moments in an infinitesimal volume of a sample under flexion.

Considering the balance of forces and moments in this volume:

$$V - (pdx) - V - dV = 0 \quad \rightarrow \quad \frac{dV}{dx} = -p \quad (24)$$

$$M - M - dM + (pdx) \cdot dx + (V + dV) \cdot dx = 0 \quad \rightarrow \quad \frac{dM}{dx} = V \quad (25)$$

By replacing equation 25 in equation 24, it is possible to come to the following equation:

$$\frac{d^2 M}{dx^2} = -p \quad (26)$$

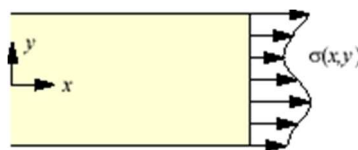


Figure 17 – Stress distribution in the transversal section of an infinitesimal volume submitted to flexion.

The stress distribution demonstrated in Figure 17 describes an aleatory dependence of the stress along the thickness of the sample, so that the moment is described as the integration between the resulting force and the dimensions of the transversal section (y and z). The equation of the resulting moment in relation to the neutral line is given by:

$$M(x) = \iint y \cdot \sigma(x, y) dydz \quad (27)$$

Replacing equation 27 in equation 26, the following equation is formed:

$$\frac{d^2}{dx^2} (\iint y \cdot \sigma(x, y) dydz) = -p \quad (28)$$

When the sample submitted to a bending test is formed by two other distinct materials, the stress distribution in the transversal section may be described by the sum of the stresses in each of the components. Disregarding the Poisson's ratio effect, the equation is given by:

$$\sigma(x, y) = \sigma_1(x, y) + \sigma_2(x, y) \rightarrow \sigma(x, y) = E_1 \cdot \varepsilon_1(x, y) + E_2 \cdot \varepsilon_2(x, y) \quad (29)$$

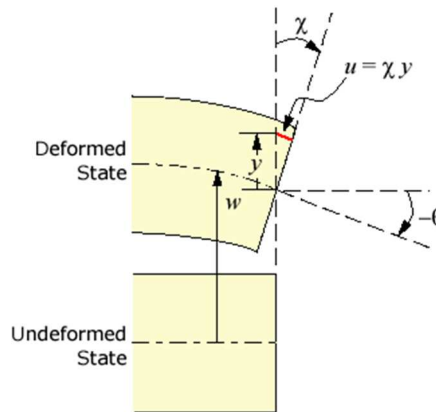


Figure 18 - Strains along x and y axes of an infinitesimal volume submitted to flexion.

Based on Figure 18, it is possible to verify that:

$$u = \chi(x) y \quad \text{and} \quad \chi(x) = \frac{dw}{dx} \quad (30,31)$$

$$\varepsilon(x, y) = \frac{du}{dx} = y \frac{d\chi}{dx} = y \frac{d^2w}{dx^2} \rightarrow \varepsilon(x, y) = y \frac{d^2w}{dx^2} \quad (32)$$

in which, w is the out-of-plane displacement (distance in which the neutral line moves away from the equilibrium); u is the displacement occurred during flexion; and χ is the rotation of the transversal section.

Therefore, based on equations 29 and 32, the following is formed:

$$\sigma(x, y) = E_1 y \frac{d^2 w}{dx^2} + E_2 y \frac{d^2 w}{dx^2} \quad (33)$$

Replacing equation 33 in equation 28:

$$\frac{d^2}{dx^2} \left[\iint y \left(E_1 y \frac{d^2 w}{dx^2} + E_2 y \frac{d^2 w}{dx^2} \right) dy dz \right] = -p \quad (34)$$

Considering that the bar is formed by two different materials such as described in Figure 11, it is possible to divide the integration for these two regions:

$$\frac{d^2}{dx^2} \left[\iint E_1 y^2 \frac{d^2 w}{dx^2} dy dz + \iint E_2 y^2 \frac{d^2 w}{dx^2} dy dz \right] = -p \quad (35)$$

The second moment of area for rectangular cross-section samples has the following form:

$$I_z = \iint y^2 dy dz \quad (36)$$

Thus, the Euler-Bernoulli equation of a bar formed by two distinct materials, disregarding the Poisson's ratio effect, is given by:

$$\frac{d^2}{dx^2} \left[E_1 \cdot I_{z_1} \cdot \frac{d^2 w}{dx^2} + E_2 \cdot I_{z_2} \cdot \frac{d^2 w}{dx^2} \right] = -p \quad (37)$$

$$\frac{d^2}{dx^2} \left[(E_1 \cdot I_{z_1} + E_2 \cdot I_{z_2}) \cdot \frac{d^2 w}{dx^2} \right] = -p \quad (38)$$

Comparing equations 38 and 23 by the equality between the stress distribution ($-p$), it is possible to estimate the effective value for the measured Young's modulus in flexion, such as:

$$E_{eff}^{flex} \cdot I_z = E_1 \cdot I_{z_1} + E_2 \cdot I_{z_2} \quad (39)$$

Despite the fact that the described equation were developed for rectangular bars, the result does not depend on this variable because even performing the transformation of coordinates to cylindrical, the final result would be the same. Therefore, considering

that for solid cylinders $I_z = \frac{\pi \cdot d^4}{64}$ and that for hollow cylinders $I_z = \frac{\pi \cdot (D^4 - d^4)}{64}$, it is possible to obtain the following correlation between the elastic moduli:

$$E_{eff}^{flex} = \frac{E_1 \cdot d^4 + E_2 \cdot (D^4 - d^4)}{D^4} \quad (40)$$

It is worth to highlight that based on this model, it is possible to visualize that the surface of a sample significantly influences the measurements taken during the flexural vibration mode. This factor will be extremely important for the cases in which the sample may present a large quantity of defects in this region.

- Developing a model for the prediction of the Young's moduli for the components of a cylindrical composite:

Based on the relations found and described by equations 22 and 40, it is possible to algebraically elaborate a two-variable system, in which by using the flexural and longitudinal elastic moduli values (E_{flex} and E_{long}) of a cylindrical composite, it is possible to calculate the Young's modulus of its components (E_1 and E_2). By simplifying the system and admitting that the longitudinal and flexural elastic moduli of materials 1 and 2 are the same, the following equations are given:

$$E_1 = \frac{E_{long}(D^2 + d^2) - E_{flex}D^2}{d^2} \quad (44)$$

$$E_2 = \frac{E_{flex}D^2 - E_{long}d^2}{(D^2 - d^2)} \quad (45)$$

Those are the main equations employed to obtain both Young's modulus values of heartwood and sapwood after characterizing only one wooden cylinder containing these two elements (case study #2). Based on the adopted convention, it is possible to conclude that E_1 will represent the Young's modulus of the heartwood, whilst E_2 will represent the Young's modulus of the sapwood.

Appendix C – Frequently asked questions (FAQ)

- What geometry should the samples be prepared in?

ASTM E1876 describes the equations for some specific geometries such as bars, cylinders, discs and rings. In general, for bars and cylinders, it is possible to characterize E and G; for discs and rings, it is possible to characterize the Young's modulus (E).

- How should the orientation of fibers be considered when characterizing and reporting results?

The characterization has to be performed and the reported results have to consider the orientation that is parallel to the length of the sample (main direction), checking if it is longitudinal, radial, tangential or a combination of directions (see chapter 3, item 3.3).

- Which value of Poisson's ratio should be used?

Considering that wood is an orthotropic material, it is not possible to obtain a reliable result for the Poisson's ratio using only this technique. Therefore, it is necessary to estimate a value for this property. Table 15 indicates possible values to be informed to the software for the elastic moduli calculation (all of them are in agreement with average values presented by different wood types). It is worth to emphasize that, in general, the sensitivity of the Young's modulus to the Poisson's ratio estimative is low.

Table 15 - Poisson's ratio for Young's modulus characterization of wooden products as a function of the sample's orientation [5].

Sample's orientation	Poisson's ratio involved	Poisson's ratio for softwood	Poisson's ratio for hardwood
Longitudinal	ν_{LT} e ν_{LR}	0.40 ± 0.05	0.43 ± 0.07
Radial	ν_{RT} e ν_{RL}	0.25 ± 0.25	0.35 ± 0.30
Tangential	ν_{TR} e ν_{TL}	0.20 ± 0.15	0.18 ± 0.15

- How should the sample be supported and excited?

The boundary conditions are determined according to the vibration mode required to measure the elastic moduli. If the goal is to obtain the Young's modulus, boundary conditions should prioritize flexural or longitudinal vibration modes. However, if the goal is to obtain the modulus of rigidity (shear modulus), boundary conditions should prioritize the torsional vibration mode (see chapter 3, item 3.2).

- How is it possible to calculate the modulus of rigidity using the effective modulus of rigidity values?

The correlation involving these properties is not trivial and it will depend on several factors. For instance, a parallel correlation of these properties is described for a wooden cylinder submitted to a torsion test [5].